

# Common Pathway for the Red Chromophore Formation in Fluorescent Proteins and Chromoproteins

Vladislav V. Verkhusha,<sup>1</sup> Dmitry M. Chudakov,<sup>2</sup>  
Nadya G. Gurskaya,<sup>2</sup> Sergey Lukyanov,<sup>2</sup>  
and Konstantin A. Lukyanov<sup>2,\*</sup>

<sup>1</sup>Department of Pharmacology  
University of Colorado Health Sciences Center  
Denver, Colorado 80262

<sup>2</sup>Institute of Bioorganic Chemistry  
Russian Academy of Sciences  
Miklukho-Maklaya 16/10  
117997 Moscow  
Russia

## Summary

The mechanism of the chromophore maturation in members of the green fluorescent protein (GFP) family such as DsRed and other red fluorescent and chromoproteins was analyzed. The analysis indicates that the red chromophore results from a chemical transformation of the protonated form of the GFP-like chromophore, not from the anionic form, which appears to be a dead-end product. The data suggest a rational strategy to achieve the complete red chromophore maturation utilizing substitutions to favor the formation of the neutral phenol in GFP-like chromophore. Our approach to detect the neutral chromophore form expands the application of fluorescent timer proteins to faster promoter activities and more spectrally distinguishable fluorescent colors. Light sensitivity found in the DsRed neutral form, resulting in its instant transformation to the mature red chromophore, could be exploited to accelerate the fluorescence acquisition.

## Introduction

Green fluorescent protein (GFP) from *Aequorea victoria* possesses the unique ability to form its internal chromophore by self-catalyzed modification of the protein chain without participation of any external cofactors except oxygen [1]. Formation of the chromophore in wild-type GFP consists of cyclization of Ser65-Tyr66-Gly67 residues followed by dehydrogenation of the Tyr66 side chain [2–6]. It results in a system of the conjugated double bonds, which is capable of absorbing violet-blue light and emitting it in the green spectral region. Recently, several fluorescent proteins (FPs) and chromoproteins (CPs) from class Anthozoa homologous to the GFP have been cloned [7–11]. Among them, the proteins with red-shifted absorbance and emission spectra are of special interest for both applied and basic science. It has been demonstrated for commercially available red fluorescent protein DsRed that a chromophore in this protein derives its spectral quality from an additional dehydrogenation of the  $\alpha$ C-N bond of Gln66, which extends the GFP-like chromophore [12–14].

The current accepted mechanism for DsRed chromophore formation consists of the formation of a GFP-like green anionic intermediate chromophore (absorption at 480 nm, emission at 500 nm), which then undergoes oxidation and turns into the mature red chromophore (absorption at 558 nm, emission at 583 nm) [12, 14–22]. This scheme was postulated on the basis of several observations. First, wild-type DsRed and many of its mutants contain green-emitting species [14–18, 20]. Second, in the course of protein maturation, the green emission appears earlier than the red one, and then gradually decreases with the same rate as the red fluorescence grows [15, 16]. Finally, the chemical structure of the red chromophore implies an extension of the GFP-like core [12].

In the present work, we studied absorption spectra during the maturation time course of DsRed and its two mutants. The data have allowed us to suggest an alternative scheme for DsRed chromophore formation. The novel scheme was found to be applicable for other red-shifted proteins such as chromoproteins asulCP [8], cgigCP, hcriCP, and far-red dimeric fluorescent protein HcRed1 [9].

## Results

### Maturation of DsRed and Its Mutants

To measure changes in the absorption curve during DsRed aging, we purified the recombinant protein from *E. coli* culture at a stage of its active growth when most of DsRed exists in an immature colorless form. The purified DsRed sample was left to mature in a cuvette of the spectrophotometer. The earliest measurement of DsRed sample produced a major absorption peak at 408 nm (B form) together with a smaller peak at 480 nm (G form) and a very small peak at 558 nm (R form) (Figure 1A). These peaks probably represent neutral and anionic GFP-like chromophores [6] and the final red chromophore form, respectively. All three peaks were rising for 4–5 hr, and later the amount of B form gradually decreased almost to zero. Peak intensities at 480 nm and 558 nm were found to grow throughout the experiment.

To exclude the influence of absorbance peaks overlay, we have decomposed the absorbance curves into Gaussian peaks (at 382 and 408 nm for the B form, at 460 and 480 nm for the G form, and at 533 and 560 nm for the R form). Figure 1B shows a time course of the areas of the decomposed peaks normalized per correspondent maximal values. These data indicate that the R form originates from the B form, whereas the G form is a dead-end product but not the intermediate form, as was suggested earlier [12, 14–22].

We also measured maturation of two DsRed mutants. The first mutant was a low-aggregating version of “fluorescent timer” [16], DsRed-E5NA (substitutions R2A, K5E, K9T, V105A, S197T) [25], the protein exhibiting spectacular transformation of green to red fluorescence.

\*Correspondence: kluk@ibch.ru

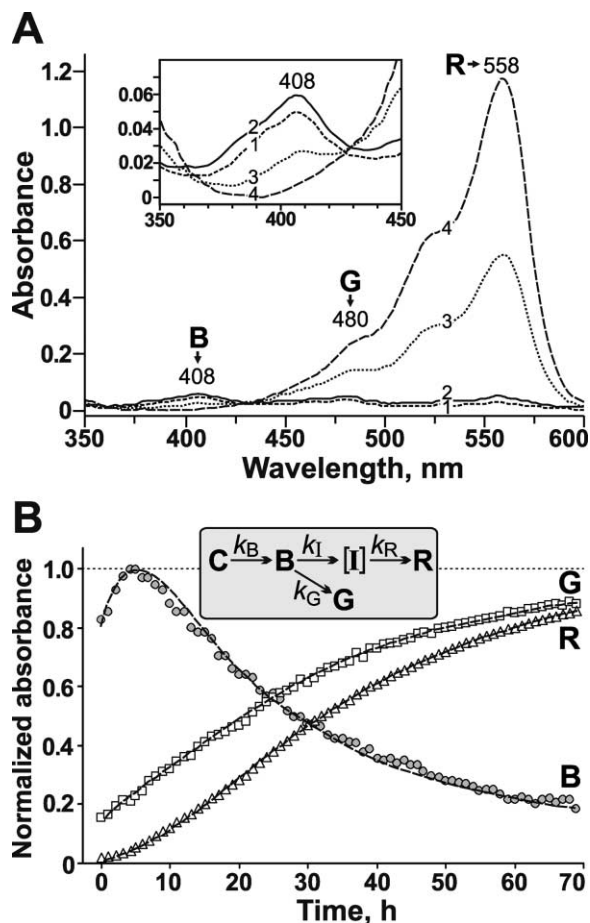


**Figure 1.** Maturation Process of DsRed Fluorescent Protein  
(A) Absorption spectra for DsRed1 at different stages of its maturation. Curves 1–4 correspond to 0, 5, 30, and 145 hr, respectively, after the first measurement of the freshly purified protein. Inset magnifies B peak.  
(B) Time course of the B, G, and R form development in DsRed (circles, squares, and triangles, respectively). Each data set was normalized per its maximal value (values at time point 5 hr for B form and at 145 hr for G and R forms). Inset shows the suggested kinetic scheme for the origination of these spectral forms from a colorless C form through the intermediate I form.  $k_B$ ,  $k_G$ ,  $k_I$ , and  $k_R$  designate rate constants for the respective reactions. Dashed line represents the fitting curves simulated in accordance with the kinetic scheme (see text for detail).

DsRed-E5NA went through absorption changes very similar to the wild-type protein DsRed. R form apparently matured through the intermediate B form, and the amount of G form never decreased in the course of maturation process (Figure 2A). Thus, an effective energy transfer from green monomers to the later-maturing red monomers within DsRed-E5NA tetramer possibly explains the observed changes in fluorescence colors [16]. Intratetramer energy migration has also been detected for the wild-type DsRed in single-molecule studies [26, 27].

The second mutant was DsRed-AG4 (substitutions V71M, V105A, S197T), which exhibits green fluorescence only [28]. Absorbance spectrum of DsRed-AG4 featured a single peak at 480 nm throughout its maturation

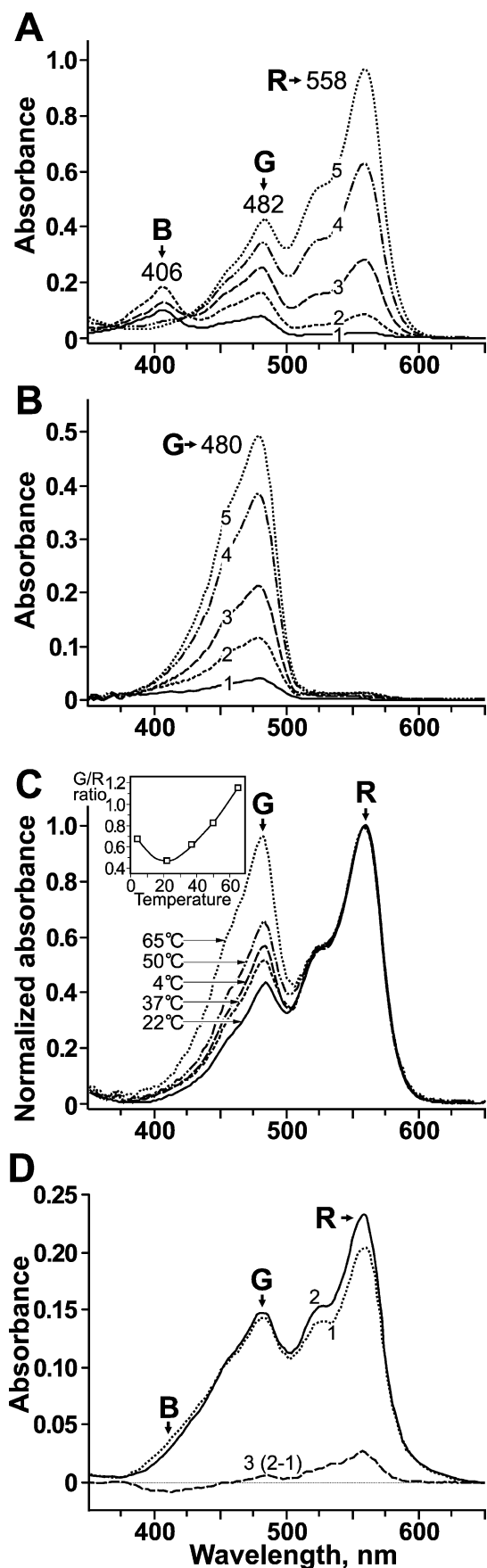
(Figure 2B). DsRed-AG4 contained negligible amounts of both B and R forms, which supports their mutual dependence hypothesis.

We further tested the influence of temperature and pH on maturation process. DsRed-E5NA mutant was selected because of its strongly pronounced G peak. Final absorption spectra for DsRed-E5NA, incubated at different temperatures in the course of maturation, showed different ratios of G and R forms (Figure 2C). The portion of G peak was minimal in the protein sample matured at room temperature, while both decreased and increased temperatures resulted in the significant growth of the G form content. No changes in the G to R form ratio were observed, even after prolonged incubation of these samples at room temperature. DsRed-E5NA protein samples that were matured at pH 5.5 or 11.5 contained larger amounts of G form as compared to the neutral pH conditions (not shown). These results could be interpreted as follows. The complex pathway for the red chromophore formation requires precise disposition of the catalytic groups [13, 14] and therefore it should be more sensitive to some external perturbations as compared to the less complicated GFP-like chromophore synthesis. That is why non-optimal temperature or pH conditions resulted in the formation of green chromophore rather than red.

Next, we studied refolding of mature DsRed-E5NA. After denaturing the sample at pH  $\sim$ 3.0, the acidity was immediately adjusted to pH 5.5 and after 1 hr incubation to pH 8.0. Thus, protein refolding occurred under mild acidic conditions, which favored the appearance of protonated chromophore state. The following incubation at neutral pH allowed us to store the protein under optimal conditions. We have found that absorption spectrum of the renatured DsRed-E5NA changed with time. Specifically, G and R peaks increased, while the shorter wavelength shoulder decreased (Figure 2D). These changes apparently imitated the normal maturation process. Similar results were obtained earlier; DsRed1 refolding from mild acid conditions led to a nearly complete elimination of the 480 nm shoulder in its absorption-excitation spectra and to a significant increase in the ratio between 558 nm and 280 nm absorption peaks [29]. These changes can be explained by protonation of the GFP-like chromophore in the acid-denatured protein (i.e., G  $\rightarrow$  B transition) followed by the formation of the red chromophore during the refolding that corresponds to B  $\rightarrow$  R transition.

#### Kinetic Scheme for the Conversions of DsRed Chromophore

To determine the kinetic scheme for DsRed chromophore formation, we performed a global fitting procedure involving all three experimental kinetic curves simultaneously (Figure 1B). For this, Gepasi simulation package was applied using a linear pathway of isomerization (closed system) model with the irreversible mass action type of kinetics [24]. The fitting procedure utilized the Levenberg-Margardt algorithm. Because protein folding and cyclization of the chromophore-forming tripeptide are significantly faster in GFP-like proteins than the subsequent chromophore oxidation step [30], we have limited our kinetic analysis to the processes follow-



ing cyclization. Four different kinetic models, (i)–(iv), were sequentially applied, assuming irreversibility of conversions for the spectral forms. Chromophore formation in the models was initiated from a spectrally undetectable C form, which represents cyclized chromophore-forming tripeptide in reduced and, therefore, colorless state. In model (i), C form is converted into either B form or G form. B form then turned into R form. In model (ii), C form is converted only into B form, which then was able to turn into either G form or R form. Although both these models described time courses for the forms B, G, and R similarly to that observed experimentally (i.e., as bell-shaped, hyperbolic, and sigmoid curves, respectively), the quality of fits for B and R forms was unsatisfactory. Therefore, we next tested models (iii) and (iv), representing modified versions of the (i) and (ii) schemas, respectively, with an intermediate I form introduced between the B and R forms. Both (iii) and (iv) fitted the experimental data significantly better. However, because our data suggested the transition between the B and G forms (see above and Figure 2D), we have finally selected model (iv) (Figure 1B, inset). Simulated curves in this model have reduced  $\chi^2$  values not exceeding  $1.2 \times 10^{-4}$  and correlation coefficients  $R^2$  above 0.995.

The fitted  $k_B$ ,  $k_G$ ,  $k_I$ , and  $k_R$  values for DsRed were  $3.31 \times 10^{-2} \text{ s}^{-1}$ ,  $6.60 \times 10^{-1} \text{ s}^{-1}$ ,  $7.13 \times 10^{-1} \text{ s}^{-1}$ , and  $7.23 \times 10^{-2} \text{ s}^{-1}$ , respectively. We have also determined the rate constants for the DsRed-E5NA maturation, which were  $1.51 \times 10^{-1} \text{ s}^{-1}$ ,  $3.46 \times 10^{-2} \text{ s}^{-1}$ ,  $4.05 \times 10^{-2} \text{ s}^{-1}$ , and  $4.79 \times 10^{-2} \text{ s}^{-1}$ , respectively. In DsRed, the B→I and B→G steps are at least 20-fold faster than the C→B and I→R reactions. Moreover, the I→R reaction seems to be a limiting step for the DsRed1 red chromophore formation, resulting in the long-living intermediate I form. In contrast, in DsRed-E5NA, the C→B reaction is the fastest step, and the B form is the long existing one. Finally, it is worth noting that current spectroscopic data do not provide insight into the nature of the intermediate I form, although it may represent neutral state of the R form or a hydroperoxide adduct; the latter has been suggested to be involved in the final DsRed chromophore oxidation step [14].

#### Fluorescent Properties of the Chromophore Forms

Fluorescence spectra for G and R forms of the wild-type DsRed protein and its mutants are well documented

Figure 2. Maturation Features of DsRed Mutants

(A and B) Absorption spectra for DsRed-E5NA (A) and DsRed-AG4 (B) at different stages of their maturation. Curves 1–5 correspond to 0, 7, 20, 40, and 150 hr (A) and 0, 10, 20, 36, and 72 hr (B) after the first measurement of the freshly purified protein.

(C) Absorption spectra for the DsRed-E5NA samples incubated at different temperatures in the course of the protein maturation. Inset shows the temperature dependence of the G form to R form spectrum areas ratio after their decomposition into Gaussian peaks.

(D) Changes of absorption spectrum for the acid-denatured DsRed-E5NA during the incubation at neutral pH. Curves 1 and 2 represent the spectrum immediately after pH neutralization and after 20 hr at pH 8.0, respectively. Curve 3 represents the differential spectrum between curves 2 and 1 that emphasizes the decrease of B form and increase of G and R forms.

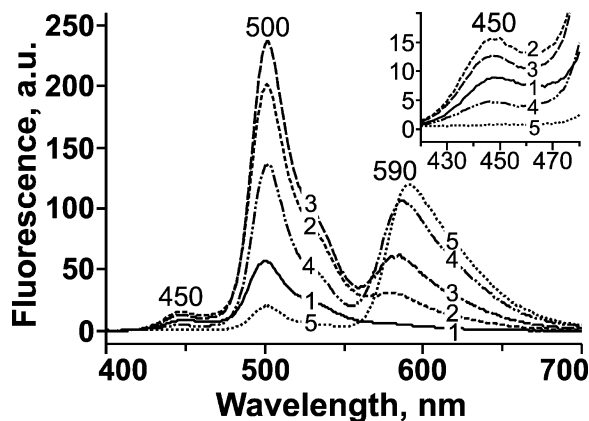


Figure 3. Fluorescence Changes in the Course of DsRed-E5NA Maturation

Emission spectra were measured using excitation at 390 nm at consecutive stages of protein maturation. Curves 1–5 correspond to 0, 9, 14, 31, and 120 hr, respectively, after the first measurement of the freshly purified protein. 450 nm, 500 nm, and 590 nm peaks represent fluorescence originating from B, G, and R forms, respectively. Inset magnifies the time changes for the B form fluorescence.

[15, 16]. In addition to the red fluorescence at 583 nm of the mature R form, G form produces green emission at about 500 nm. We examined fluorescence changes during maturation of DsRed-E5NA. Because the ratio between green and red fluorescence reflects the age of DsRed-E5NA (“young” protein produces green fluorescence while the “old” protein is mainly red), this mutant was found to be a useful tool for visualization of up- and downregulation of the target promoters and the relative age of cells, intracellular organelles, and proteins [16, 31–33]. We have found that excitation of B form in DsRed-E5NA at about 400 nm produces weak blue fluorescence. Its emission peak at 450 nm was clearly detected at the early stages of the protein maturation and then gradually decreased down to zero (Figure 3).

#### A Three-Color Fluorescent Timer Expressed in Living Cells

To figure out whether fluorescence of the B form can be detected by fluorescence microscopy, we have expressed DsRed-E5NA in human HEK293 cells. To synchronize induction, DsRed-E5NA was expressed under the Tet-On inducible system. Standard DAPI, FITC, and Cy3 filter sets were used. Distinct blue and green fluorescence were visible after 6–8 hr, whereas cells with all three colors (blue, green, and red), appeared only 12–14 hr after induction (Figure 4). In DAPI channel, blue DsRed-E5NA fluorescence was up to one order higher than the intracellular autofluorescence. The use of a spectrally optimized filter for B form instead of the DAPI filter could further increase this contrast. The ability to detect B form by standard fluorescence methods allows us to assay target protein twice as soon as in the case of G and R forms tracking and extends the number of sequentially changeable color hues: blue, white, yellow, and red (Figure 4, overlay).

#### Light Sensitivity of the B Form

In the course of the experiments described, we noticed sensitivity of the B form to the illuminating light. Illumination through the 100× objective at DAPI channel using a powerful 175 W Xenon lamp for more than 10 s resulted in a detectable decrease of the blue and the respective increase in red fluorescence. We studied this light-induced B→R transition for DsRed1 in detail. First, action spectrum of this transition was determined, in which we measured the relative increase in the red fluorescence of overnight grown *E. coli* colonies expressing DsRed1 after irradiation at the different wavelengths (Figure 5A). We found that two wavelengths, 410 and 380 nm, are most effective for the light-induced conversion. Finally, we studied the correspondence of the light-induced conversion to light intensity at the fixed wavelength (Figure 5B). The dependence was linear, suggesting that this transition is a one-photon process.

#### Light-Induced Fluorescence Acquisition In Vivo

Light-induced B→R transition can be exploited to accelerate the fluorescence acquisition for DsRed variants and other red fluorescent proteins. Indeed, at early stages of DsRed expression in *E. coli*, we were able to increase the red fluorescence signal up to 4.4-fold by 2–3 min intense irradiation with 405 nm light using a fluorescent stereomicroscope (not shown). To further verify this feature, mammalian cells expressing DsRed2 (substitutions R2A, K5E, K9T, V105A, I161T, S197A) 18 hr after transfection were irradiated using DAPI filter and 100× objective and then imaged in Cy3 channel. Red fluorescence intensity increased 1.6- to 2.0-fold and reached a plateau within 90–120 s for different cells (Figures 5C and 5D). The pre-exposure to far-UV-violet light resulted in a visible increase of red fluorescence without affecting cellular morphology.

#### Maturation of the GFP-like Chromoproteins

We also studied maturation process for three chromoproteins (cgigCP, hcricP, and asulCP) recently cloned from *Condylactis gigantea*, *Heteractis crispa*, and *Anemonia sulcata*, respectively [8, 9]. The earliest measured immature cgigCP sample demonstrated a major absorption peak at 400 nm (i.e., B form) and a minor peak at 568 nm (R form) (Figure 6, curve 1). Both peaks increased slightly over a short period of time (Figure 6, curve 2), followed by the B form’s gradual decrease to zero (Figure 6, curves 3–5), while R form matured to its maximal value at 568 nm. Thus, the B form peak appeared to convert into R form peak with an isosbestic point at 465 nm. Chromoproteins asulCP and hcricP, as well as dimeric far-red fluorescent mutant, HcRed1, exhibited generally the same maturation behavior as cgigCP detected by their absorption spectra (not shown). The G forms were not observed in absorption spectra of these proteins.

#### Discussion

The currently accepted conclusion about the formation of the red fluorophore within DsRed through a green-emitting intermediate was mainly based on the gradual

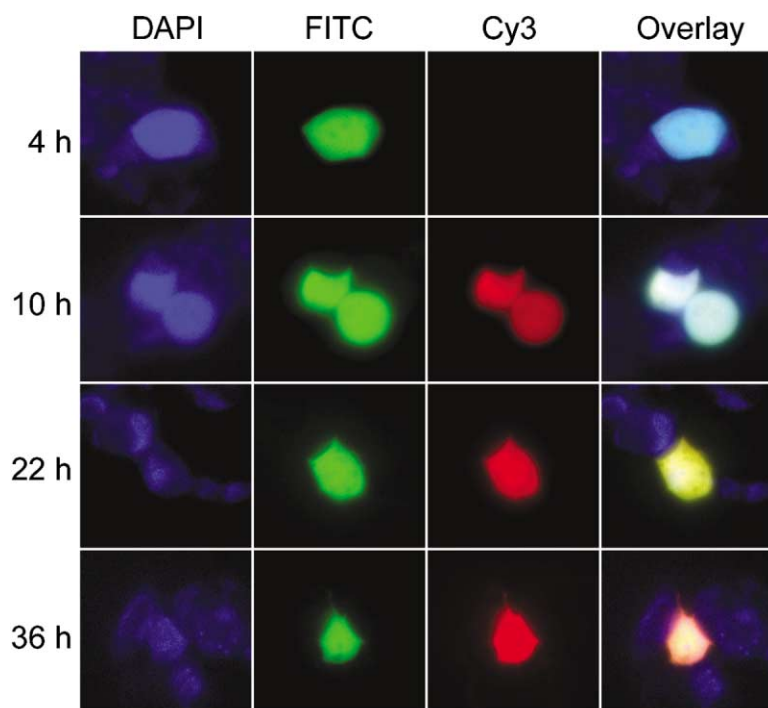


Figure 4. Visualization of Emission Colors of Fluorescent Timer DsRed-E5NA in Human HEK293 Cells

Pulse-chase induction of DsRed-E5NA under the control of the Tet-On system was used to synchronize expression. Fluorescence images in the respective wavelength channels (DAPI, FITC, and Cy3) and their overlay of the representative living cells are shown. Tet-On induction was performed for 4 hr, and the time values at the left indicate the time after the end of Tet-On induction.

and proportional transformation of the green fluorescence into red in the course of DsRed's mutant maturation [15, 16]. In fact, these fluorescent color changes are explained by efficient FRET between green and red monomers within DsRed tetramers, but not the chemical transformation of the green into the red chromophore. True amounts of each spectral form can only be estimated from absorption spectra. In the present work, we showed that the B form is the intermediate while both G and R forms are the terminal ones. The changes in the DsRed absorption spectra have been described by Wiehler and coworkers [18]. However, based on logically incorrect normalization of all spectra to the red absorption at 558 nm, the authors have made an incorrect

conclusion about relative decrease of the green absorbing peak and therefore transformation of green into red chromophore during DsRed maturation.

Origination of the R form exclusively from the B form easily explains the fact of completely mature wild-type DsRed, as well as its mutants, containing some portion of the green-emitting chromophore, which never converts into red chromophore. Within the old concept, this fact was perplexing. Therefore, it was proposed that the transformation of green to red chromophore could occur at some stage of protein folding process only [19]. Also, it was suggested that the equilibrium between green and red DsRed chromophores was due to reversibility of the final oxidation step or reversible hydration of

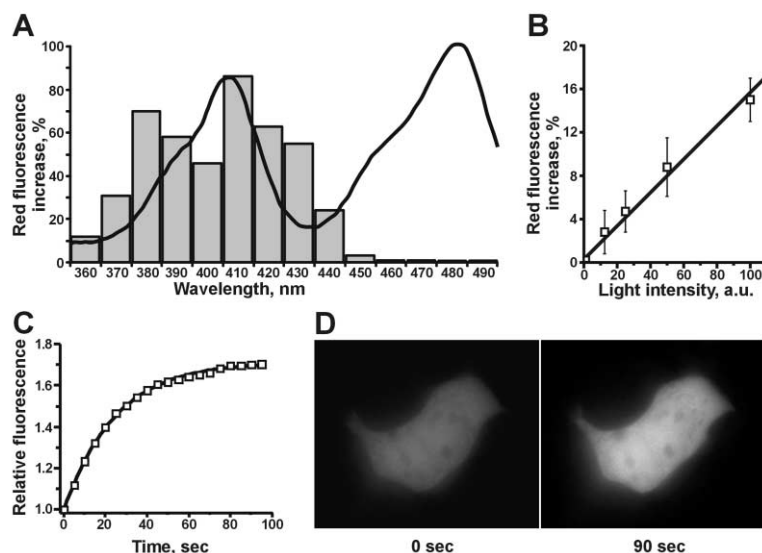


Figure 5. Light-Induced Conversion of DsRed Variants

(A) Action spectrum is presented as a histogram showing relative increase of the immature DsRed1 red fluorescence after its irradiation with light of the defined wavelengths. Fluorescence intensity before irradiation was taken for 100%. Immature DsRed1 absorption spectrum is shown for comparison.

(B) Linear dependence of the increase in DsRed1 fluorescence from the intensity of inducing light (360–400 nm).

(C and D) Acceleration of DsRed2 maturation in living human HEK293 cells by pre-irradiation with UV-violet light. Time course for the red fluorescence growth is shown. The total intensity of cell fluorescence prior to light treatment was set as 1 (C). The image of representative cell before (0 s) and 90 s after the irradiation through DAPI filter (D) is shown.

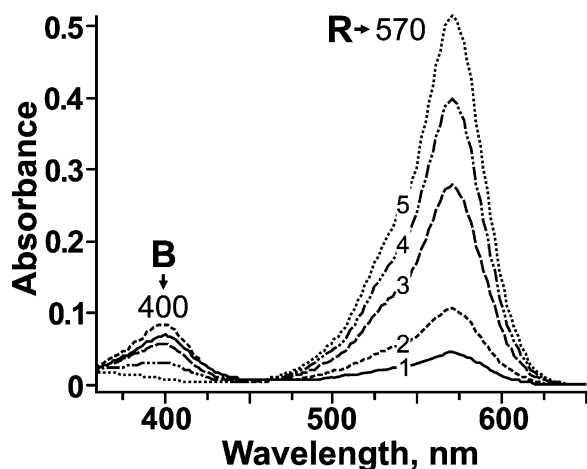


Figure 6. Maturation Process of the Chromoprotein cgigCP

Absorption spectra at the consecutive stages of the protein maturation at room temperature (22°C) are shown. Curves 1–5 correspond to 0, 1, 2.5, 4, and 20 hr, respectively, after the first measurement of the freshly purified protein. Here, R forms (~570 nm) apparently originate from B form (400 nm), and G form (~480 nm) is absent.

an acylimine group of the chromophore by internal water molecule in DsRed protein [20].

Most likely, the B form corresponds to a neutral state and the G form to the anionic state of GFP-like chromophore [6]. Thus, dehydrogenation of Gln66 in DsRed and formation of the red chromophore state can occur only in the protonated form of the GFP-like intermediate (B form). Why does the red chromophore originate from neutral but not from anionic form? A possible explanation can be proposed on the basis of the available crystallographic data and quantum-chemical calculations. Yarbrough and coworkers suggested that the crucial step in the oxidation of a GFP-like intermediate into mature DsRed chromophore is the deprotonation of the  $\alpha$ C of Gln66, resulting in the formation of a highly reactive carbanion [14]. On the other hand, calculation of atomic charges for the GFP chromophore has shown a significant charge difference on the correspondent carbon atom in the anionic and neutral states [34]. In the anionic chromophore this carbon is almost uncharged, while in the neutral chromophore it carries a significant negative charge ( $-0.39$ ) and its proton has a positive charge ( $+0.22$ ). Consequently, these partial charges should greatly decrease the activation energy required for the proton abstraction and carbanion formation. Therefore, the scheme outlined in Figure 7 for the formation of DsRed chromophore is suggested. The backbone cyclization at positions 66–68 is followed by the dehydrogenation of a Tyr67 methylene bridge. Prior to dehydrogenation, Tyr67 apparently exists in a protonated state, and therefore the neutral GFP-like chromophore should be formed first. This reasoning completely corresponds to the experimental data demonstrating the B form appearance earlier than the others. Then, proton transfer could result in a formation of the anionic GFP-like chromophore (G form). Alternatively, the neutral chromophore could serve as a substrate in a complex pathway toward red chromophore formation. A  $\alpha$ C-H bond of

Gln66 is highly polarized in the neutral chromophore state. Due to this polarization, oxidation of the Gln66  $\alpha$ C-N bond through the carbanion intermediate might effectively occur, resulting in the formation of the mature red chromophore (R form). Kinetic modeling suggests the existence of an intermediate I form(s) between the B and R forms. We believe it could be the hydroperoxide adduct as proposed by Yarbrough and coworkers [14] or simply the protonated state of the red chromophore.

Particular attention should be paid to relations between neutral and anionic chromophore states. We aver that there is no equilibrium between the neutral and the anionic states of the GFP-like chromophore in DsRed, although in other proteins it could exist. In other words, in DsRed the G form does not convert back into the B form. Otherwise, we would observe slow transformation of the G peak into the R peak that has never been detected even after prolonged storage of DsRed and its mutants at various temperatures. Also, emission, excitation, and absorption spectra for mature DsRed were found to be stable between pH 5 and 11 [15, 17]. Explanation for such strong stabilization of the anionic chromophore can be derived from DsRed crystal structure [13, 14]. Indeed, the number of hydrogen bonds and particularly a charge-charge interaction with the neighboring Lys163 ensures the chromophore's phenolate oxygen to be charged at all time in the mature DsRed protein.

We believe that neutral GFP-like chromophore can exist in the immature DsRed protein only. It has been shown for GFP that the chromophore's phenolic oxygen moves for 14 Å within the protein during the chromophore formation [35]. A similar Tyr67 movement possibly occurs in DsRed as well. It is reasonable to suggest that the chromophore-stabilizing network could form after the Tyr67 displacement only, and this is a time-dependent process. Therefore, the observed B→G transition reflects the formation of the chromophore environment, which irreversibly stabilizes the anionic state. The similar stabilizing network possibly appears after the red chromophore formation.

Our data allow for the suggestion of a novel interpretation of some DsRed mutagenesis results and a rational design strategy to achieve the full maturation of the red chromophore. The amino acid mutations described to favor the formation of the protonated chromophore's phenolate would improve the maturation of red fluorescent proteins. Indeed, several substitutions at positions 163 and 197 close to the chromophore, such as K163M, K163Q, S197I, S197A, and S197Y, found originally by random mutagenesis of DsRed [28, 36–38], caused faster and complete maturation of DsRed.

It is more difficult to explain the influence of V71M substitution resulting in pure green fluorescent phenotype in the DsRed-AG4 mutant. It was proposed that the larger Met71 produces a distortion of chromophore environment and thus should block the final chromophore oxidation [28]. If this is the case, the accumulation of B form, at least at some maturation stages, must be observed. Our data show that AG4 exhibits negligible amount of the B and R forms. Thus, V71M mutation somehow inhibits the formation but not the oxidation of the B form. According to the DsRed crystal structure,

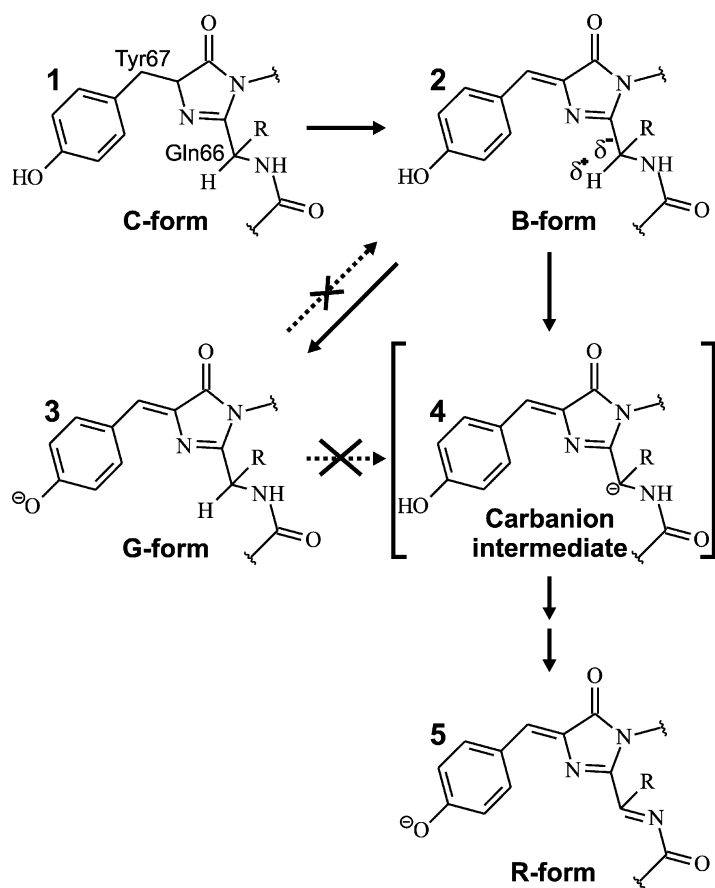


Figure 7. Suggested Scheme for DsRed Chromophore Formation

Structure 1 represents cyclization of the protein backbone into five-membered heterocycle due to bond formation between carbonyl carbon of Gln66 and amide nitrogen of Gly68. Then, oxidation of Tyr67  $\alpha$ C- $\beta$ C bond occurs and GFP-like chromophore in protonated (neutral) state appears (structure 2). After that, the chromophore can follow two mutually exclusive ways. First, it can fall into anionic state (structure 3). In contrast to GFP, there is no equilibrium between these states in DsRed. Second, the structure 2 can be converted into mature red chromophore. In the neutral state,  $\alpha$ C of Gln66 carries partial negative charge and its hydrogen carries partial positive charge (designated as  $\delta^-$  and  $\delta^+$ , respectively). This bond polarization greatly facilitates the formation of unstable carbanion intermediate (structure 4) where  $\alpha$ C of Gln66 possesses a charge of  $-1$  due to proton abstraction. Following the intermediate stage, mature red chromophore containing double bond between  $\alpha$ C and amide nitrogen of Gln66 is formed (structure 5). In contrast, anionic GFP-like chromophore (structure 3) carries a practically nonpolarized  $\alpha$ C-H bond of Gln66. Thus, it never converts into carbanionic intermediate compound (structure 4) because the required activation energy for the proton abstraction is too high.

Val71 and Lys70 side chains are almost anticollinear. We believe that the larger Met71 residue could displace adjacent Lys70 toward the chromophore's phenolate, resulting in the fast deprotonation of the chromophore. In compliance with this argument, the introduction of a smaller side chain at position 71, such as substituting alanine for valine, led to drastic decrease of the green component in the excitation spectrum [36].

As compared to DsRed, its mutant E5NA contains larger amounts of the G form. Thus, its key substitution, S197T, should support formation of the deprotonated green chromophore. Because Ser197 lies in the closest proximity to the chromophore's phenolate oxygen but is turned away from the chromophore [14], there is no H bond between Ser197 and chromophore's phenolate. It can be proposed that due to tight residue package within DsRed, the larger Thr197 adopts a conformation where its OH group forms an H bond with the chromophore, thus stabilizing its deprotonated state.

The observed light sensitivity of DsRed maturation process is possibly biologically significant. According to the photoprotective function of fluorescent proteins in corals suggested by Salih and coworkers [39], excessive sunlight results in an increase in the production of endogenous GFP-like proteins. However, accumulation and maturation are slow processes. Possibly, the instantaneous light-activated maturation of GFP-like proteins allows for the faster adaptation to strong sunlight irradiation in tropical waters that corals and corallimorphs inhabit.

How widespread is the chromophore formation mechanism presented here? In addition to DsRed, three other chromoproteins and a far-red fluorescent mutant HcRed1 clearly demonstrate the transformation of the intermediate B form into the mature R form. Moreover, in contrast to DsRed, no spectral form absorbing at 480–500 nm (G form) was detected in these proteins. Recently, Ando and coworkers have described a photoconvertible fluorescent protein, Kaede, from the stony coral *Trachyphyllia geoffroyi* [11]. This protein forms its mature red chromophore from the neutral GFP-like chromophore with an absorption maximum at 380 nm only in response to irradiation with 350–400 nm light. Red-emitting chromophore within Kaede is formed as a result of an unusual cleavage of the protein backbone between the amide nitrogen and the  $\alpha$ C carbon of His62 (this residue corresponds to Gln66 in DsRed) and subsequent formation of a double bond between  $\alpha$ C and  $\beta$ C of His62 [21]. In spite of different chromophore structures, one can see clear similarities between the maturation processes of Kaede and DsRed. In both proteins, mature R forms originate from B forms, and B forms are light sensitive; they can be fast transformed into R forms by one-photon absorption processes. Mechanisms of the photo-induced chromophore formation in these RFPs are still unclear. We believe that the photon energy may allow overpassing an activation barrier in these reactions. Further time-resolved spectroscopic characterization could shed light on these processes.

Finally, the data presented reveal new useful features

of the widely used fluorescent tags commercially available from BD Biosciences Clontech. First, the presence of the additional blue color in Fluorescent Timer protein (i.e., DsRed-E5) makes it possible to visualize its earliest maturation stages. This will expand areas of its application toward detection of faster promoter activities and distinguishing more populations of aging organelles or differentiating cells in vivo. Second, it was demonstrated that maturation of commonly used DsRed1 and DsRed2 markers could be significantly accelerated. Soon after the expression start, the red fluorescence is weak, so one can easily enhance fluorescence signal several-fold by brief irradiation of expressing cells through the conventional DAPI channel.

## Significance

**Chromophore formation in the members of the GFP family proteins represent a unique example of self-catalyzed reaction without requiring accessory cofactors, external enzymatic catalysis, or substrates other than molecular oxygen. Here, we describe a novel mechanism for the chromophore maturation in DsRed, as well as other red fluorescent proteins and chromoproteins with red-shifted absorption. This scheme seems to be common for all known red-shifted proteins, in spite of clear differences between the final structures of their chromophores. We demonstrated the phenomenon of light-induced DsRed maturation, which possibly plays a role in nature for fast adaptation of corals to strong tropical sunlight. In addition to theoretical interest, the present data can be used in practice. We suggested a way to expand the application range of so-called fluorescent timers for detection of faster promoter activities and for distinguishing more populations of aging organelles or differentiating cells in vivo. Finally, our results suggest a novel rational design strategy to achieve complete maturation of red fluorescent proteins.**

## Experimental Procedures

### Plasmid Construction and Protein Expression

For bacterial expression, the full-length coding regions of the proteins' cDNA were amplified using specific primers and cloned into the pQE30 vector in *Bam*HI and *Hind*III sites (Qiagen). The proteins fused to an N-terminal polyhistidine tag were expressed in *E. coli* XL1-Blue host (Invitrogen) and purified using TALON metal-affinity resin (Clontech). For expression in eukaryotic cells, pDsRed2-C1 vector (Clontech) was used. Also, a nonaggregating DsRed-E5NA mutant bearing N-terminal mutations reducing its cytotoxicity was amplified as *Age*I-*Not*I fragment and cloned into the respective sites of pOSTet-7.81 vector (gift of Y. Miwa), resulting in pOSTet-DsRed-E5NA plasmid.

### Characterization of Protein Spectral Properties

Absorption spectra during maturation of the fluorescent proteins and chromoproteins were recorded with Beckman DU520 UV/VIS Spectrophotometer followed by subtraction of the scattered light. Varian Cary Eclipse Fluorescence Spectrophotometer was used for measuring excitation-emission spectra. For maturation kinetics measurements, freshly transformed *E. coli* cells were spread onto 3–4 Petri dishes and grown at 30°C overnight (under these conditions the protein maturation is usually far from completion). Then, cells were suspended in phosphate-buffered saline (PBS) (pH 7.0) and disrupted by sonication. Recombinant proteins were purified from

soluble fraction by TALON resin (Clontech). Absorption or fluorescence spectra for maturing proteins were collected at 60 min intervals at room temperature (22°C). Microcal Origin software was used to decompose absorption spectra into Gaussian peaks before and after conversion of the wavelengths to wave numbers [23]. For kinetic simulation of DsRed maturation and determination of the kinetic rate constants, Gepasi package was applied [24].

### Maturation Kinetic Dependence upon Temperature and pH

To measure temperature dependence, immature DsRed-E5NA protein sample was divided onto five tubes, and each of them was incubated at a defined temperature (4°C, 22°C, 37°C, 50°C, or 65°C). For pH dependence, the immature DsRed-E5NA protein sample was buffered either by 50 mM citric-phosphate (pH 5.5) or 50 mM Tris-Cl (pH 11.5) buffers. Absorption spectra were recorded upon complete maturation. For DsRed-E5NA denaturation-renaturation studies, protein sample matured at 4°C was treated with 1 M HCl up to the complete loss of red coloration. Then, pH was immediately adjusted to pH 5.5 by citric-phosphate buffer. Irreversibly denatured protein was pelleted by 5 min centrifugation at 10,000 × g. After 1 hr incubation at pH 5.5, the sample was neutralized by Tris-Cl buffer to pH 8.0. Absorption spectra were measured immediately after neutralization, and in 20 hr, about one-third of the initial protein amount was found to be renatured under these conditions.

### Light Sensitivity of Maturing DsRed

To study wavelength dependence for light-induced changes of the red fluorescence, single bacterial colonies expressing DsRed1 24 hr after transformation (growth at 30°C) were irradiated for 20 s with Nikon Eclipse TE100 inverted microscope equipped with monochromator (10 nm bandwidth) through 40× air objective using 175 W Xenon lamp as the source. The emission was detected through the standard Cy3 filter set (Chroma). The images before and after irradiation were acquired by CCD camera (Princeton Instruments) and quantified by SlideBook software. For dependence from illuminating light intensity, the colonies were irradiated on the similar microscope equipped with a set of neutral filters on the excitation 100 W mercury source. Irradiation was performed for 60 s through 10× air objective using standard DAPI filter set (Chroma). The average values for 5 colonies are presented for both wavelength and light intensity dependencies.

### Mammalian Cell Culture

Human epithelial kidney cells HEK293 were obtained from ATCC and cultured in standard Dulbecco's modified MEM medium (Invitrogen) supplemented with 10% FBS (Sigma) at 37°C. Cells were transfected with pOSTet-DsRed-E5NA plasmid using Effectene reagent (Qiagen), and stable preclonal mixture was selected with 1.5 mg/ml of Geneticin (Invitrogen) for 10 days. The antibiotic-selected cells were grown to 50% confluence on coverslips coated with human fibronectin (Sigma), and induction of DsRed-E5NA expression was induced by 1 μg/ml of doxycycline (Sigma) for 4 hr followed by its extensive washing and addition of a fresh medium.

### Fluorescent Microscopy and Imaging

The fluorescence images of living cells at the respective time points were acquired using Nikon Eclipse TE300 inverted microscope equipped with 60× PlanApo oil immersion objective lens, cooled CCD SensiCam QE camera (Cooke, Germany), and dual filter wheels, and controlled by SlideBook software (Intelligent Imaging Innovation). 2 × 2 binning mode, and 500, 10, and 10 ms exposure times were used for DAPI (Ex. 380BP20 nm, Em. 460BP50 nm), FITC (Ex. 480BP40 nm, Em. 535BP40 nm), and Cy3 (Ex. 535BP50 nm, Em. 610BP75 nm) filters (Chroma), respectively. To study light-induced changes of the red fluorescence, living HEK293 cells 24 hr after transfection with standard pDsRed2-C1 plasmid (BD Clontech) were sequentially irradiated through 100× PlanApo oil immersion objective using DAPI filter for 5 s followed by 5 ms imaging through Cy3 filter. For each time point, an average cellular intensity was quantified on pixel basis followed by subtraction of the background.



### Acknowledgments

We thank Dr. Y. Miwa for pOSTet-7.81 vector. This work was supported in part by the grants from European Office of Aerospace Research and Development under ISTC partner project 2325 and Russian Academy of Sciences for the program "Physicochemical Biology." V.V.V. acknowledges support from the grants NIH/NIDA DA14204-01 and INIA AA13489.

Received: January 22, 2004

Revised: April 6, 2004

Accepted: April 7, 2004

Published: June 25, 2004

### References

1. Heim, R., Prasher, D.C., and Tsien, R.Y. (1994). Wavelength mutations and posttranslational autoxidation of green fluorescent protein. *Proc. Natl. Acad. Sci. USA* **91**, 12501–12504.
2. Shimomura, O. (1979). Structure of the chromophore of *Aequorea* green fluorescent protein. *FEBS Lett.* **104**, 220–222.
3. Cody, C.W., Prasher, D.C., Wastler, W.M., Prendergast, F.G., and Ward, W.W. (1993). Chemical structure of the hexapeptide chromophore of the *Aequorea* green-fluorescent protein. *Biochemistry* **32**, 1212–1218.
4. Ormo, M., Cubitt, A.B., Kallio, K., Gross, L.A., Tsien, R.Y., and Remington, S.J. (1996). Crystal structure of the *Aequorea victoria* green fluorescent protein. *Science* **273**, 1392–1395.
5. Yang, F., Moss, L.G., and Phillips, G.N., Jr. (1996). The molecular structure of green fluorescent protein. *Nat. Biotechnol.* **14**, 1246–1251.
6. Niwa, H., Inouye, S., Hirano, T., Matsuno, T., Kojima, S., Kubota, M., Ohashi, M., and Tsuji, F.I. (1996). Chemical nature of the light emitter of the *Aequorea* green fluorescent protein. *Proc. Natl. Acad. Sci. USA* **93**, 13617–13622.
7. Matz, M.V., Fradkov, A.F., Labas, Y.A., Savitsky, A.P., Zaraisky, A.G., Markelov, M.L., and Lukyanov, S.A. (1999). Fluorescent proteins from nonbioluminescent Anthozoa species. *Nat. Biotechnol.* **17**, 969–973.
8. Lukyanov, K.A., Fradkov, A.F., Gurskaya, N.G., Matz, M.V., Labas, Y.A., Savitsky, A.P., Markelov, M.L., Zaraisky, A.G., Zhao, X., Fang, Y., et al. (2000). Natural animal coloration can be determined by a nonfluorescent green fluorescent protein homolog. *J. Biol. Chem.* **275**, 25879–25882.
9. Gurskaya, N.G., Fradkov, A.F., Terskikh, A., Matz, M.V., Labas, Y.A., Martynov, V.I., Yanushevich, Y.G., Lukyanov, K.A., and Lukyanov, S.A. (2001). GFP-like chromoproteins as a source of far-red fluorescent proteins. *FEBS Lett.* **507**, 16–20.
10. Wiedenmann, J., Schenk, A., Rucker, C., Girod, A., Spindler, K.D., and Nienhaus, G.U. (2002). A far-red fluorescent protein with fast maturation and reduced oligomerization tendency from *Entacmaea quadricolor* (Anthozoa, Actinaria). *Proc. Natl. Acad. Sci. USA* **99**, 11646–11651.
11. Ando, R., Hama, H., Yamamoto-Hino, M., Mizuno, H., and Miyawaki, A. (2002). An optical marker based on the UV-induced green-to-red photoconversion of a fluorescent protein. *Proc. Natl. Acad. Sci. USA* **99**, 12651–12656.
12. Gross, L.A., Baird, G.S., Hoffman, R.C., Baldridge, K.K., and Tsien, R.Y. (2000). The structure of the chromophore within DsRed, a red fluorescent protein from coral. *Proc. Natl. Acad. Sci. USA* **97**, 11990–11995.
13. Wall, M.A., Socolich, M., and Ranganathan, R. (2000). The structural basis for red fluorescence in the tetrameric GFP homolog DsRed. *Nat. Struct. Biol.* **7**, 1133–1138.
14. Yarbrough, D., Wachter, R.M., Kallio, K., Matz, M.V., and Remington, S.J. (2001). Refined crystal structure of DsRed, a red fluorescent protein from coral, at 2.0-Å resolution. *Proc. Natl. Acad. Sci. USA* **98**, 462–467.
15. Baird, G.S., Zacharias, D.A., and Tsien, R.Y. (2000). Biochemistry, mutagenesis, and oligomerization of DsRed, a red fluorescent protein from coral. *Proc. Natl. Acad. Sci. USA* **97**, 11984–11989.
16. Terskikh, A., Fradkov, A., Ermakova, G., Zaraisky, A., Tan, P., Kajava, A.V., Zhao, X., Lukyanov, S., Matz, M., Kim, S., et al. (2000). Fluorescent timer: protein that changes color with time. *Science* **290**, 1585–1588.
17. Mizuno, H., Sawano, A., Eli, P., Hama, H., and Miyawaki, A. (2001). Red fluorescent protein from *Discosoma* as a fusion tag and a partner for fluorescence resonance energy transfer. *Biochemistry* **40**, 2502–2510.
18. Wiehler, J., von Hummel, J., and Steipe, B. (2001). Mutants of *Discosoma* red fluorescent protein with a GFP-like chromophore. *FEBS Lett.* **487**, 384–389.
19. Remington, S.J. (2002). Negotiating the speed bumps to fluorescence. *Nat. Biotechnol.* **20**, 28–29.
20. Bevis, B.J., and Glick, B.S. (2002). Rapidly maturing variants of the *Discosoma* red fluorescent protein (DsRed). *Nat. Biotechnol.* **20**, 83–87.
21. Mizuno, H., Mal, T.K., Tong, K.I., Ando, R., Furuta, T., Ikura, M., and Miyawaki, A. (2003). Photo-induced peptide cleavage in the green-to-red conversion of a fluorescent protein. *Mol. Cell* **12**, 1051–1058.
22. Miyawaki, A., Nagai, T., and Mizuno, H. (2003). Mechanisms of protein fluorophore formation and engineering. *Curr. Opin. Chem. Biol.* **7**, 557–562.
23. Lakowicz, J.R. (1999). Principles of Fluorescence Spectroscopy, 2nd edition (New York: Kluwer Academic).
24. Mendes, P. (1997). Biochemistry by numbers: simulation of biochemical pathways with Gepasi 3. *Trends Biochem. Sci.* **22**, 361–363.
25. Yanushevich, Y.G., Staroverov, D.B., Savitsky, A.P., Fradkov, A.F., Gurskaya, N.G., Bulina, M.E., Lukyanov, K.A., and Lukyanov, S.A. (2002). A strategy for the generation of non-aggregating mutants of Anthozoa fluorescent proteins. *FEBS Lett.* **511**, 11–14.
26. Cotellet, M., Hofkens, J., Habuchi, S., Dirix, G., van Guyse, M., Michiels, J., Vanderleyden, J., and de Schryver, F.C. (2001). Identification of different emitting species in the red fluorescent protein DsRed by means of ensemble and single-molecule spectroscopy. *Proc. Natl. Acad. Sci. USA* **98**, 14398–14403.
27. Garcia-Parajo, M.F., Koopman, M., van Dijk, E.M., Subramaniam, V., and van Hulst, N.F. (2001). The nature of fluorescence emission in the red fluorescent protein DsRed, revealed by single-molecule detection. *Proc. Natl. Acad. Sci. USA* **98**, 14392–14397.
28. Terskikh, A.V., Fradkov, A.F., Zaraisky, A.G., Kajava, A.V., and Angres, B. (2002). Analysis of DsRed Mutants. Space around the fluorophore accelerates fluorescence development. *J. Biol. Chem.* **277**, 7633–7636.
29. Vrzheschch, P.V., Akovbian, N.A., Varfolomeyev, S.D., and Verkhusha, V.V. (2000). Denaturation and partial renaturation of a tightly tetramerized DsRed protein under mildly acidic conditions. *FEBS Lett.* **487**, 203–208.
30. Reid, B.G., and Flynn, G.C. (1997). Chromophore formation in green fluorescent protein. *Biochemistry* **36**, 6786–6791.
31. Duncan, R.R., Greaves, J., Wiegand, U.K., Matskevich, I., Bodammer, G., Apps, D.K., Shipston, M.J., and Chow, R.H. (2003). Functional and spatial segregation of secretory vesicle pools according to vesicle age. *Nature* **422**, 176–180.
32. Wiegand, U.K., Duncan, R.R., Greaves, J., Chow, R.H., Shipston, M.J., and Apps, D.K. (2003). Red, yellow, green go! A novel tool for microscopic segregation of secretory vesicle pools according to their age. *Biochem. Soc. Trans.* **31**, 851–856.
33. Bertera, S., Geng, X., Tawadrous, Z., Bottino, R., Balamurugan, A.N., Rudert, W.A., Drain, P., Watkins, S.C., and Trucco, M. (2003). Body window-enabled in vivo multicolor imaging of transplanted mouse islets expressing an insulin-Timer fusion protein. *Biotechniques* **35**, 718–722.
34. Helms, V., Winstead, C., and Langhoff, P.W. (2000). Low-lying electronic excitations of the green fluorescent protein chromophore. *J. Mol. Struct.* **506**, 179–189.
35. Barondeau, D.P., Putnam, C.D., Kassmann, C.J., Tainer, J.A., and Getzoff, E.D. (2003). Mechanism and energetics of green fluorescent protein chromophore synthesis revealed by trapped intermediate structures. *Proc. Natl. Acad. Sci. USA* **100**, 12111–12116.
36. Campbell, R.E., Tour, O., Palmer, A.E., Steibach, P.A., Baird,

- G.S., Zacharias, D.A., and Tsien, R.Y. (2002). A monomeric red fluorescent protein. *Proc. Natl. Acad. Sci. USA* 99, 7877–7882.
37. Verkhusha, V.V., Otsuna, H., Awasaki, T., Oda, H., Tsukita, S., and Ito, K. (2001). An enhanced mutant of red fluorescent protein DsRed for double labeling and developmental timer of neural fiber bundle formation. *J. Biol. Chem.* 276, 29621–29624.
38. Knop, M., Barr, F., Riedel, C.G., Heckel, T., and Reichel, C. (2002). Improved version of the red fluorescent protein (drFP583/DsRed/RFP). *Biotechniques* 33, 592–602.
39. Salih, A., Larkum, A., Cox, G., Kuhl, M., and Hoegh-Guldberg, O. (2000). Fluorescent pigments in corals are photoprotective. *Nature* 408, 850–853.